Available online at www.sciencedirect.com
SCIENCE DIRECT®
Catalysis Today 101 (2005) 245–252
CATALYSIS TODAY
www.elsevier.com/locate/cattod

Enhanced photocatalytic degradation of maleic acid by Fe(III) adsorption onto the TiO_2 surface

Maria Isabel Franch *, José A. Ayllón, José Peral, Xavier Domènech

Departament de Química, Universitat Autònoma de Barcelona, 08193 Bellaterra, Barcelona, Spain

Available online 23 March 2005

Abstract

The role of Fe(III) on the TiO_2-assisted photocatalytic degradation of maleic acid has been investigated. The study on the kinetics of the removal of organic matter, as well as the identification of all the stable mineralization intermediates, demonstrates that the presence of Fe(III), adsorbed onto the TiO_2 surface, renders a more efficient process through a cleaner mineralization pathway compared to bare TiO_2. Furthermore, the behaviour of the system does not depend on the iron source. On the other hand, the study of the Fe(III) influence on the interaction of maleic acid with TiO_2 in the solid phase, by means of ATR–FT-IR technique, has been performed. From all the reported results, it is concluded that the Fe(III) effects are mainly due to surface phenomena. The enhanced photocatalytic activity is interpreted under different perspectives, including adsorbed Fe–maleic complexes, enhanced adsorption of oxygen and lower geminate recombination yields.

Keywords: Photocatalysis; Maleic acid; Surface modification; Fe(III)

1. Introduction

The increasing volume of wastewaters released to the environment containing non-biodegradable pollutants requires the development of new powerful, clean and safe decontamination technologies. In this sense, heterogeneous photocatalysis has emerged as a helpful tool. Heterogeneous photocatalysis is based on the photogeneration of reductant and oxidant species able to promote the mineralization of organic matter. The great power of this technique for the elimination of pollutants in the aqueous phase has already been widely demonstrated [1–3]. An additional reason for advocating for heterogeneous photocatalysis is that it fits the Green Chemistry postulates [4]. TiO_2, the most widely used photocatalyst for such application, is a cheap and harmless material that, besides, can be recovered and reused. Furthermore, heterogeneous photocatalysis can work by using sunlight, which is a renewable energy source [5,6].

Yet, the implementation of heterogeneous photocatalysis for the treatment of wastewaters at large scale is still a challenging matter of investigation. The work of several research groups deals with the enhancement of the TiO_2 response to visible light, in order to develop a system able to operate efficiently taking advantage of a major percentage of the sunlight [7,8]. Also, the relatively low mineralization rates need to be improved.

A wide number of non-biodegradable pollutants contain one or more aromatic rings in their chemical structure. It is well known that the oxidative cleavage of the aromatic ring leads to the formation of short-chain carboxylic acids [9]. In this sense, the study of the photocatalytic degradation of short-chain organic acids would be helpful. It might be thought that, as the toxicity of such mineralization intermediates is usually low, they should not be a matter of environmental concern, since they could be eliminated by biological treatment [10]. However, this kind of compounds shows a great affinity to the TiO_2 surface compared to the adsorption tendency of aromatic species [11]. Hence, the fastest the carboxylic acids are eliminated, the easiest the degradation of the parent aromatic pollutants would be. Besides that, the ability of carboxylic acids to form coordination complexes with transition metals must be considered, since such process might stabilize harmful species in the aqueous phase.

* Corresponding author. Tel.: +34 935812919; fax: +34 935812920.
E-mail address: maribel@qf.uab.es (M.I. Franch).

0920-5861/$ – see front matter © 2005 Elsevier B.V. All rights reserved.
doi:10.1016/j.cattod.2005.03.007

We have chosen maleic acid (MA) as a model of short-chain carboxylic acids. It has been detected by several authors as an intermediate generated during the photocatalytic degradation of aromatic pollutants [12–14]. Also, MA is released to the environment from textile, lubricant additives, drugs and polymer manufacturing [15,16].

We have already reported a comprehensive study of the photocatalytic degradation of MA by using heterogeneous photocatalysis (TiO_2 + UV) [17]. Since it is well known that Fe(III)–carboxylic complexes are easily photo-oxidised, we have studied the Fe(III)-mediated homogeneous photocatalytic degradation of MA as well [18]. Our results indicated that, for MA mineralization, heterogeneous photocatalysis is certainly less efficient than homogeneous iron-mediated photodegradation. Nevertheless, Fe(III)-mediated homogeneous photocatalysis does not appear to be as suitable as heterogeneous photocatalysis for the treatment of a wide class of pollutants. Besides that, the catalyst recovery, which is generally easier for the heterogeneous than for homogeneous catalysis technologies, is one of the drawbacks of water purification techniques based on the use of Fe(III) or Fe(II) in aqueous solution [19].

The aim of this work is to study the possibility of taking advantage of the benefits of TiO_2 and Fe(III) photocatalysts. The literature results concerning the Fe(III) effects on the photocatalytic degradation processes have been contradictory. This controversy regards the marked influence of experimental parameters such as Fe(III) concentration and pH values on the iron speciation. Low Fe(III) concentration and acid pH values have been used to avoid the metal ion detrimental effects, often ascribed to short-circuiting reactions, that produce electron–hole recombination, hydroxides precipitation over the TiO_2 surface and UV light dispersion or filtration [20]. In this sense, MA photocatalytic degradation assays have been performed by using TiO_2 previously modified by Fe(III) adsorption from diluted aqueous solution at acid pH values. It is noteworthy that the Fe(III) loading technique used in this work avoids thermal treatment and, hence, excludes the additional energy and economical cost that TiO_2 thermal doping implies. The reported results of the mineralization of MA in the presence of Fe(III) allow us to conclude that iron adsorption over TiO_2 modifies the mineralization pathway of MA and leads to improved mineralization yields.

2. Experimental

2.1. Reagents

All chemicals mentioned hereafter were, at least, of reagent grade and used as received. Solutions were prepared with water purified in a Millipore Milli-Q system. TiO_2 Degussa P25 (80% anatase −20% rutile, 59 $m^2\,g^{-1}$, non-porous) was used as the photocatalyst.

2.2. Photocatalytic and adsorption studies

Photocatalytic and adsorption experiments were performed in a 0.4 L cylindrical Pyrex reactor provided with a thermostatic jacket to keep the temperature at 25 ± 0.1 °C. During the assays, the aqueous suspensions were magnetically stirred and air was continuously bubbled through them. The initial pH values were adjusted to 2.8 ($HClO_4$ or NaOH) for both photocatalysis and adsorption studies.

In the heterogeneous photocatalytic experiments (named TiO_2 + UV experiments in the text), 0.600 g of TiO_2 powder were added to 0.400 L of MA aqueous solution at 1.00×10^{-3} mol L^{-1} initial concentration. The aqueous suspension was kept in the dark, until adsorption equilibrates (30 min), before irradiation started. In the heterogeneous photocatalytic assays with Fe(III) (named TiO_2/Fe + UV in the text), 0.600 g of TiO_2 powder were added to 0.200 L of a Fe(III) aqueous solution at 0.200×10^{-3} mol L^{-1} initial concentration (prepared by using $FeCl_3$ or $Fe_2(SO_4)_3$ as the iron source). Once adsorption equilibrium of Fe(III) over TiO_2 was achieved, 0.200 L of MA aqueous solution at 2.00×10^{-3} mol L^{-1} initial concentration were added. The aqueous suspension was kept in the dark for another period until equilibrates. Irradiation of the suspensions was carried out by using a medium pressure mercury vapour lamp Philips HPK 125 W as light source. The lamp was placed in a water-cooled Pyrex jacket that filtered both UV ($\lambda < 290$ nm) and IR radiations. At different irradiation times, samples were removed from the reactor and filtered through a 0.45 μm pore size nylon filter before analysis.

Samples for ATR–FT-IR measurements were prepared following the procedure performed in the dark and described above. Once adsorption equilibrium was achieved, the suspension was filtered through a 0.45 μm pore size nylon membrane. The obtained solid was dried at room temperature. Once the ATR spectrum of such solid sample (named TiO_2/MA or TiO_2/Fe/MA in the text) was measured, the sample was extended over a watch glass dish under UV irradiation. The ATR–FT-IR spectrum of the irradiated sample was registered after 30 min of light exposure. The TiO_2/Fe, TiO_2/Fe/malonic and TiO_2/formic samples were prepared by the same procedure described above.

Photocatalysis assays by using reused TiO_2/Fe catalyst were performed to test the catalyst recovery. At the end of the TiO_2/Fe-mediated photocatalytic mineralization of MA (when no organic carbon is detected), the catalyst was separated from the aqueous phase by filtration through a 0.45 μm pore size nylon membrane. The solid was washed with acidified water ($HClO_4$, pH 2.8) and partially dried at room temperature. After this, the photocatalytic degradation of MA was performed as described above for the TiO_2 + UV system, by using the recovered TiO_2/Fe catalyst instead of bare TiO_2.

2.3. Analytical methods

The concentration of organic carboxylic acids was measured by HPLC analysis. The HPLC system was constituted by an LC-10 AT VP pump (Shimadzu), a UV–vis absorbance detector (Applied Absorbance Biosystems 759A) adjusted at 210 nm, and an HP 3394A integrator. An Aminex-87-H column (300 mm × 7.8 mm), working at room temperature, was used as the stationary phase. The mobile phase was a 0.005 mol L^{-1} H_2SO_4 aqueous solution working at isocratic flow rate of 0.75 mL min^{-1}. Total organic carbon (TOC) determination was carried out with a TOC-5000 SHIMADZU Total Carbon Analyser provided with a NDIR detector. Both the HPLC and TOC measurements have been replicated at least two times. The error has never been above 5%.

The aqueous iron concentration analyses were performed by the *o*-fenantroline method, based on measurement at 510 nm of the absorbance of the [Fe(*o*-fen)$_3$] complex. UV–vis spectra were registered with an HP-8453 diode array spectrometer [21].

ATR–FT-IR measurements of TiO_2 solid samples were performed with a Bruker apparatus (Tensor model equipped with MKII Golden Gate).

3. Results

3.1. Adsorption and kinetic studies in the aqueous phase

The amount of Fe(III) and MA adsorbed onto TiO_2 has been measured, at the same experimental conditions used in the photocatalysis assays, by using either $FeCl_3$ or $Fe_2(SO_4)_3$ as iron sources ($[Fe(III)(aq.)]_0 = 1.00 \times 10^{-4}$ mol L^{-1}; $[TiO_2] = 1.50$ g L^{-1}; pH_0 2.8). Once adsorption equilibrium is achieved, the remaining concentration of iron in aqueous solution does not depend on the iron salt being used. The amount of Fe(III) retained by the catalyst is 0.4 wt.%. Several authors have found that the photocatalytic activity of TiO_2 is considerably increased by using similar amounts of Fe(III) as doping agent [22,23]. In our case, however, the economical cost due to firing treatment is avoided. Moreover, the possibility of phase transformations (anatase → rutile) catalysed by the presence of iron at high temperatures, that would render a lower photoactivity, is avoided [22,24]. Nevertheless, in the present study, there is no Fe(III) on the bulk of the TiO_2 material and, thus, it would be more accurate to express the amount of Fe(III) in terms of surface concentration instead of the weight percentage value. The surface coverage can be calculated taking into account the amount of Fe(III) adsorbed over a given mass of catalyst and considering the specific surface value of the material (59 m^2 g^{-1}). The coverage of the TiO_2 surface is about 0.7 Fe(III) molecule per nm^2 (at the experimental conditions given above). For MA ($[MA]_0 = 1.00 \times 10^{-3}$ mol L^{-1}; $[TiO_2] = 1.50$ g L^{-1}; pH_0 2.8), the surface coverage is 0.9 molecule per nm^2 over TiO_2, and 0.6 molecule per nm^2 over TiO_2/Fe. At these conditions, the main species of Fe(III) and MA in the aqueous solution are the $[Fe(H_2O)_5OH]^{2+}$ complex and the monoprotonated form of maleate, respectively. The competition of these species for the same adsorption sites should render a lower MA coverage over TiO_2/Fe than the reported value, unless the organic diacid binds to adsorbed Fe(III) species. The binding of MA to adsorbed Fe(III) could improve the photocatalytic degradation yields, since our previous results indicate that the Fe(III)–maleate complex formation leads to efficient mineralization of MA [18].

The TiO_2/Fe-mediated photocatalytic degradation rate of MA in aqueous media has been studied ($[MA]_0 = 1.00 \times 10^{-3}$ mol dm^{-3}, and pH_0 2.8). In these assays, Fe(III), when present, has been loaded over the TiO_2 surface from two different sources, sulphate or chloride salts (see Fig. 1). The heterogeneous photocatalytic process by using bare TiO_2 (TiO_2 + UV) and the Fe(III)-mediated homogeneous photocatalytic degradation of maleic acid are also shown. The reported results clearly show that the heterogeneous system works much better when TiO_2/Fe instead of bare TiO_2 is used. Besides, it is noteworthy that the TiO_2/Fe system appears to behave in a more consistent manner, compared to the Fe(III) + UV assays, when changes on the nature of the inorganic anions are involved.

At first, it might be reasonably assumed that the improvement of the TiO_2/Fe + UV process, compared to TiO_2 + UV assays, is due to the ability of Fe(III) to promote the homogeneous photocatalytic mineralization of MA in irradiated aqueous solutions [18]. Nevertheless, this explanation does not stand up if we consider the different behaviour of Fe(III) + UV and TiO_2/Fe + UV regarding salt effects. The influence of the nature of the inorganic anions appears to arise on the strength of the changes that they promote in the coordination sphere of the ferric complexes

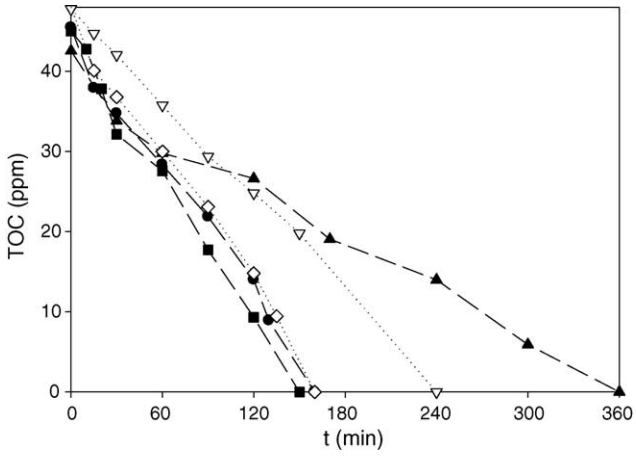

Fig. 1. Total organic carbon (TOC) measurements along irradiation time during the photocatalytic degradation of maleic acid (MA) ($c_0 = 1.00 \times 10^{-3}$ mol L^{-1}); pH_0 2.8; $T = 25$ °C: (▲) TiO_2 + UV; (▽) Fe(III) + UV ($FeCl_3$); (◇) Fe(III) + UV ($Fe_2(SO_4)_3$); (●) TiO_2/Fe + UV ($FeCl_3$); (■) TiO_2/Fe + UV ($Fe_2(SO_4)_3$).

[18,25–27]. Hence, in the TiO_2/Fe + UV assays, the photoactive ferric species must be the same, regardless the presence of chloride or sulphate anions. This could be interpreted to mean that MA binds adsorbed Fe(III) without leaving available positions for sulphate or chloride ligands. However, from the lack of effects due to iron source, in the TiO_2/Fe(III) + UV assays, it might be reasonably assumed that iron participates in the photocatalytic degradation process while chemisorbed over the titania surface.

3.2. Studies on the mineralization intermediates

To go deeply into the role of Fe(III), the nature of the intermediates generated during heterogeneous photocatalytic mineralization of MA, as well as their contribution to TOC measurements, have been investigated. We have already reported analogous studies in the case of the Fe(III)-mediated homogeneous photocatalytic degradation of MA [18]. In this previous work we found that formic acid was the main contribution to measured TOC during the mineralization process.

The results of the study on the TiO_2-mediated mineralization of MA are presented in Fig. 2a. At the earlier mineralization stages, acrylic and formic acids are the only detected intermediates. Later on, malonic and acetic acids become the main contribution to the measured TOC. Malic and oxalic acids formation is also observed but at very low concentrations (below the analytical quantification limit (1×10^{-5} mol L^{-1})). Fumaric acid is also detected during the irradiation process, although not being a mineralization intermediate but a *cis–trans* isomerization product of MA.

The concentration profiles depicted in Fig. 2b correspond to the study on the intermediates generated along the mineralization process of maleic acid in the TiO_2/Fe + UV system. These results are comparable when $Fe_2(SO_4)_3$ is used instead of $FeCl_3$ as iron source. As can be seen, malonic and formic acids are the only detected mineralization intermediates. Fumaric acid formation is observed but at lower concentration (below the quantification limit (5×10^{-6} mol L^{-1})) than in the absence of Fe(III). It could be thought that, the reason why neither acetic nor acrylic acids are detected in this case is that these carboxylic acids could form easily photodegradable iron-complexes. However, since the Fe(III)-mediated photodegradation of acetic or acrylic is not faster than the observed kinetics for malonic or formic acids [18], such explanation does not appear to apply.

It is worth mentioning that, in the studies on the mineralization intermediates shown above (Fig. 2), the calculated TOC nearly matches the measured TOC. This can be taken to mean that there are no other stable species in solution different from those that appear in the graph. One of the streaking aspects that firstly arises, from comparison of the results shown in Fig. 2, is that just a small amount of Fe(III) is required to greatly enhance the TOC removal rate at the same time that the number of detected intermediates is lowered. Nevertheless, the mineralization rates observed in the TiO_2/Fe + UV assays are comparable to those for Fe(III)-mediated homogeneous mineralization of MA, when $Fe_2(SO_4)_3$ is used as iron source (see Fig. 1). On balance, the main difference between the TiO_2/Fe + UV and the $Fe_2(SO_4)_3$ + UV assays is the detection of significant quantities of malonic acid in the former case, while formic acid is detected in both of them.

Scheme 1 shows the proposed main mineralization pathways of MA that could explain the different behaviour of the TiO_2 + UV and TiO_2/Fe + UV systems [17,18,28,29]. The first step on the degradation of MA, step 1 in Scheme 1, is proposed to be a photo-Kolbe process, that is the oxidative decarboxylation of MA leading to a carbon-centred radical. Such process would initiate the oxidative degradation of the studied diacid for both the TiO_2 + UV [17] and the TiO_2/Fe + UV photocatalytic process. Once oxidation of MA occurs, and before decarboxylation process, the radical

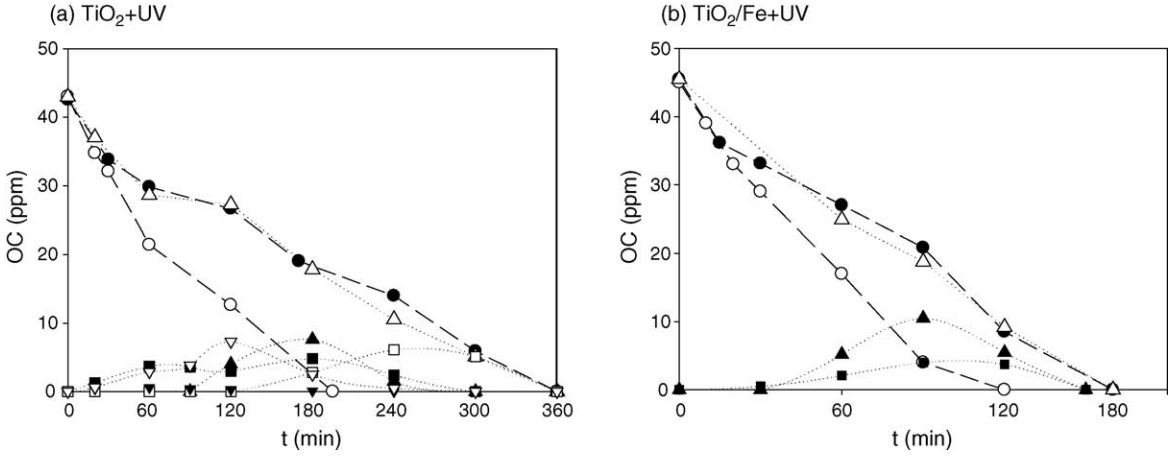

Fig. 2. Time course of the remaining concentration of maleic acid (MA) as well as the generated intermediates during photocatalytic degradation of MA, where $[MA]_0 = 1.00 \times 10^{-3}$ mol L^{-1}; $[TiO_2] = 1.50$ g L^{-1}; pH_0 2.8; $T = 25.0$ °C and $[FeCl_3]_0 = 1.00 \times 10^{-4}$ mol L^{-1} used for iron loading: (a) TiO_2 + UV and (b) TiO_2/Fe + UV: measured total organic carbon (TOC) (●), MA (○), malonic (▲), formic (■), acetic (□), fumaric (▼), acrylic (▽), MA + intermediates (△). The concentration of MA and intermediates are expressed in organic carbon (OC) units.

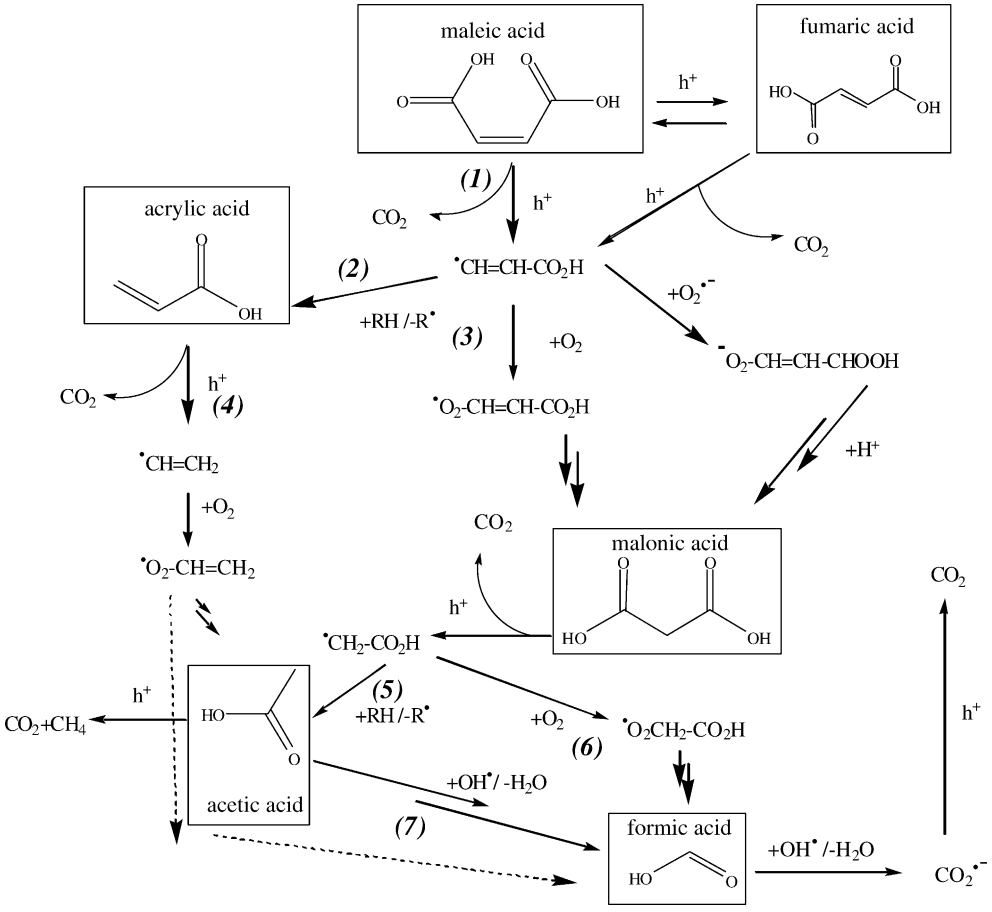

Scheme 1. Proposed mechanism for TiO_2 heterogeneous photocatalytic degradation of maleic acid (see Refs. [17,18,28,29]). The h^+ symbol indicates the oxidation reaction of the organic molecule with a photogenerated hole on TiO_2 but also through a LMCT process to Fe(III) adsorbed over the TiO_2 surface. The scheme does not include the acid–base equilibria or adsorption–desorption processes.

cation of MA, with a lower rotation barrier than the parent compound, could lead to fumaric acid formation. Alternatively, the isomerization process can occur through MA radical anion, formed by the electron transfer of e_{cb}^- to MA [30].

In the case of TiO_2 + UV assays, the mineralization of maleic acid is proposed to occur through the steps on 1, 2 (or 3), 4 and 7 (or 5 and 7) in Scheme 1, accordingly to the concentration profiles during the mineralization process (see Fig. 2a). At the first stages of the degradation process, the carbon-centred radical formed in step 1 would evolve, mainly, to acrylic acid formation (see Fig. 2a). The acrylic acid mineralization could occur through acetic acid or, alternatively, by means of a peroxide intermediate that would evolve to formic acid. Once MA concentration has been lowered enough (see Fig. 2a), the malonic acid instead of acrylic acid formation, step 3 instead of step 2, becomes more important. Malonic acid degradation would occur mainly through a photo-Kolbe process followed by the hydrogen abstraction reaction (step 5).

In the case of TiO_2/Fe + UV assays, maleic acid mineralization process would follow, preferentially, the pathway shown in the centre of Scheme 1 (through steps 3 and 6). As can be seen, the pathways that might lead to the formation of malonic acid production need O_2 or $O_2^{\bullet-}$ to be involved. Also, it is significant that malonic acid evolution to acetic acid does not need oxygen or superoxide participation, while direct evolution to formic acid does. Finally, it must be said that, analogously to step 3, an alternative pathway by means of superoxide could occur for step 6. To summarize, the overall picture shows as the iron loading favours those pathways that need O_2 or $O_2^{\bullet-}$ participation.

3.3. ATR–FT-IR studies

In Scheme 1, the TiO_2 and TiO_2/Fe-mediated photocatalytic degradation of MA is proposed to be initiated mainly by a photo-Kolbe process, that is, the direct electron transfer, from chemisorbed MA to TiO_2, coupled to decarboxylation process. The nature of the binding between the diacid and the TiO_2 surface would affect the efficiency of the electron transfer process and, as a consequence, the observed degradation kinetics.

ATR–FT-IR studies are very useful to characterize the nature of the chemical interaction between organic acids chemisorbed on TiO_2 [11]. In this work, we use this

technique as a helpful tool to investigate whether Fe(III) modifies MA interaction with the catalyst surface. The ATR–FT-IR spectrum of Fe(III) adsorbed onto TiO_2, by using either $FeCl_3$ or $Fe(SO_4)_3$ as iron source, has been measured (not shown). No differences have been found among these spectra and the bare TiO_2 spectrum except for very small new bands in the OH stretching bands zone. Since these bands disappear when MA is adsorbed over the catalyst, they might correspond to Fe–OH vibration modes.

Fig. 3 shows the measured infrared spectra of MA adsorbed onto bare TiO_2 (TiO_2/MA) and onto TiO_2 in the presence of preadsorbed Fe(III) as well (TiO_2/Fe/MA). The vibration mode assignment of the infrared absorption bands of MA species is reported in Table 1. The broad bands at 1636 and 1640 cm^{-1} missing in this table can be ascribed to the scissoring vibration of adsorbed water molecules [31].

The infrared spectrum of the TiO_2/MA sample contains the bands at 1559 and 1421 cm^{-1} due to the antisymmetric and symmetric stretching modes of CO_2^- group. The appearance of such bands may indicate that MA binds TiO_2 surface in a bridging bidentate fashion. On the other hand,

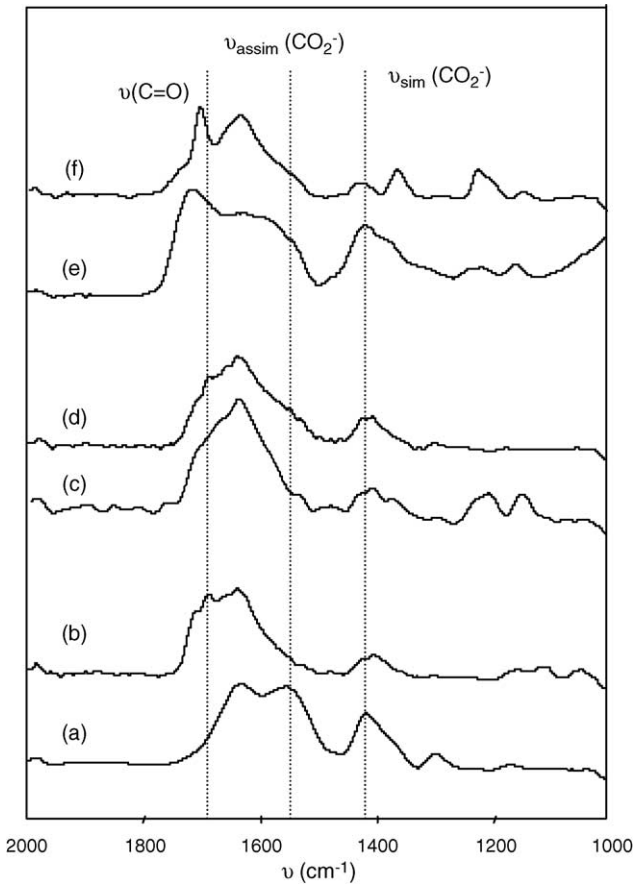

Fig. 3. ATR–FT-IR spectra of maleic acid (MA), malonic and acrylic acids adsorbed onto TiO_2 or TiO_2/Fe: (a) TiO_2/MA; (b) TiO_2/Fe/MA; (c) TiO_2/MA after 30 min of UV irradiation; (d) TiO_2/Fe/MA after 30 min of UV irradiation; (e) TiO_2/acrylic; (f) TiO_2/Fe/malonic. The samples where prepared from aqueous solution where [organic acid] = 1.00×10^{-3} mol L^{-1}, [TiO_2] = 1.5 g L^{-1}, pH 2.8 and [Fe(III)] = 100×10^{-4} mol L^{-1}.

Table 1
Wave numbers of absorption maxima in the infrared spectra of maleic acid (MA) (1×10^{-1} mol L^{-1}) and maleate (1×10^{-1} mol L^{-1}) in aqueous solution and MA adsorbed to TiO_2 (TiO_2/MA) and TiO_2 + Fe(III) (TiO_2/Fe/MA) from an aqueous solution where [MA] = 1×10^{-3} mol L^{-1}, [TiO_2] = 1.5 g L^{-1}, pH 2.8 and [Fe(III)] = 1×10^{-4} mol L^{-1}

MA (aq.)[a]	Maleate (aq.)[a]	TiO_2/MA	TiO_2/Fe/MA	Assignment (a, b)
1711			1711, 1689	ν(C=O)[a]
1626, 1567				ν(C=C)[a]
	1553	1559		$\nu_{as}(CO_2^-)$[a]
1476				
	1430	1421		$\nu_s(CO_2^-)$[a]
	1413			δ(CH)[a]
			1409	
1387				
1383				
		1304		δ(CH)[a]
1236				
1178	1187	1174		
			1160	ν_{as}(CO)[b]
			1114	ν_s(CO)[b]
			1052	δ(CH)[b]

[a] See [32].
[b] Attempted assignment considering typical values.

when MA chemisorption takes place in the presence of iron, the C=O vibrations modes (1711 and 1689 cm^{-1}) are observed. Therefore, the binding of MA onto TiO_2/Fe must be through monodentate carboxylic groups, probably by means of ester-like linkage of the protonated form. Anyway, the multiplet at 1700 and 1400 cm^{-1} can be due, among other reasons, to the presence of different types of C(=O)O–M or C(=O)O(H)–M groups, where M could be Fe(III) or Ti(IV) [32]. Definitely, the observed differences between TiO_2/MA and TiO_2/Fe/MA spectra allow us to conclude that the coordination mode of MA adsorbed onto the semiconductor surface becomes different in the presence of iron.

ATR–FT-IR studies with irradiated samples have also been performed. Although the identification of all the observed infrared bands is out of the scope of this work, these studies have been aimed to ascertain whether Fe(III) adsorption onto titania can promote a different reaction pathway of MA in the solid phase. The TiO_2/MA and TiO_2/Fe/MA solid samples have been irradiated for 30 min (see c and d) spectra in Fig. 3. The spectrum 3c shows as, in the absence of iron, after irradiation, the bands at 1559 and 1421 cm^{-1} appear to be just a shoulder of some new bands, and also the band at 1304 cm^{-1} has nearly disappeared. This result indicates MA degradation. The appearance of the new bands at 1365, 1211 and 1152 cm^{-1} could be related with acrylic acid formation (see Fig. 3e). In the presence of Fe(III), the irradiation of the organic acid chemisorbed to the catalyst surface promotes the decrease of the C=O band at 1711 cm^{-1}, and those at 1114 and 1052 cm^{-1} as well. The bands at 1690, 1660 and 1411 cm^{-1} could be related to malonic acid formation (see Fig. 3f). However, since the spectrum is quite noisy, the observed vibration bands can be hardly assigned. That might be due to a lower amount of

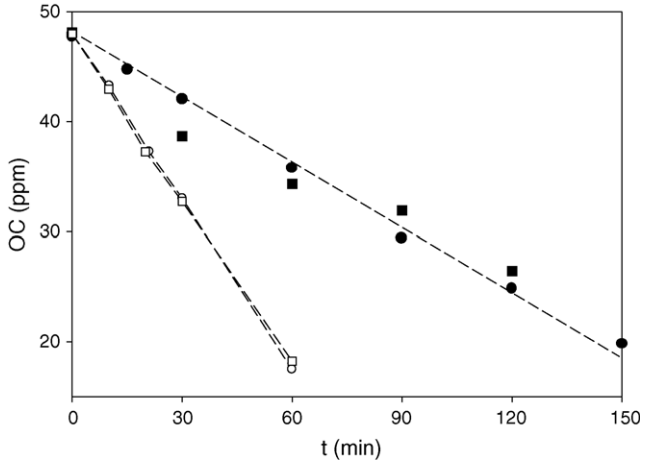

Fig. 4. Time course of the remaining concentration of maleic acid (MA) (empty symbols) as well as the measured total organic carbon (TOC) (filled symbols) during UV-illumination of an aqueous suspension where: $[MA]_0 = 1.00 \times 10^{-3}$ mol L^{-1}, pH_0 2.8; $T = 25.0$ °C. The catalyst was TiO_2/Fe prepared from $[TiO_2]_0 = 1.5$ g L^{-1} and $[Fe_2(SO_4)_3]_0 = 1.00 \times 10^{-4}$ mol L^{-1}. First run: circles; second run (catalyst reused): squares. The concentration of MA is expressed in organic carbon (OC) units.

remaining organic species over the titania surface, after irradiation, when Fe(III) is present. Certainly, although the ATR–FT-IR measurements in the solid phase cannot be directly related with the photocatalytic process in the aqueous media, it is noteworthy that the FT-IR spectra presented agree with the behaviour of the studied system in the aqueous phase.

3.4. Catalyst reutilization studies

The benefits of Fe(III) adsorption over the TiO_2 surface have been clearly demonstrated. However, in order to test whether the Fe(III) adsorption is a suitable immobilization method, TiO_2/Fe(III) recovery studies have been performed. The results shown in Fig. 4 correspond to the TiO_2/Fe catalyst reutilization assays. A second run was performed with the same TiO_2 used in the first run, that was separated from the aqueous phase by filtration once no TOC was detected in the aqueous solution (see Section 2). The ATR–FT-IR analysis of the catalyst surface (not shown) demonstrated that the surface was clean at that time. Hence, truly mineralization is achieved. The recurrence of the evolution of TOC measurements along irradiation time presented in Fig. 4 makes clear that the amount of iron chemisorbed over the TiO_2 surface is enough to play its beneficial effect.

4. Discussion

There are several approaches to explain the results reported in this paper. In one hand, Fe(III) adsorption create new acidic sites on the surface that would increase oxygen adsorption. Such effect can be related to the higher yields of those pathways that need O_2 or $O_2^{\bullet -}$ participation. However, the effect of Fe(III) on MA adsorption must also be considered. The ATR–FT-IR results indicate that when Fe(III) has been loaded over TiO_2 before MA adsorption, the organic diacid binds TiO_2 by means of ester-like linkage, whereas without Fe(III), MA binds TiO_2 surface in a bridging bidentate fashion. Obviously, the different coordination of the diacid might imply the different molecular orbital pattern and, hence, the different electron transfer kinetics. Besides, it is expectable that MA radical, formed by direct reaction with a photogenerated hole, would be more easily removed from the surface in the TiO_2/Fe case, since MA coordination does not seem to imply the four oxygen atoms of the molecule. This is meant to be that geminate recombination yield would be lowered in the presence of iron, rendering to improved mineralization yields. The isomerization of MA to fumaric acid could occur through the reorganisation of the oxidised form of the diacid before decarboxylation process, followed by the back electron transfer to the diacid, a geminate recombination process [17,33]. The lower degree of isomerization of maleic to fumaric acid in the case of TiO_2/Fe + UV compared to TiO_2 + UV assays agrees with the view of the Fe(III) role in the geminate recombination yields (in the former case fumaric acid is only detected at the first stages, when MA concentration is high enough). Analogous explanation can be considered when *cis–trans* isomerization might follow the radical anion pathway proposed by Oh et al. [30]. Finally, the photoactivity of Fe–MA complexes must be considered [18,22,23,34–36]. MA could be oxidised by means of LMCT to adsorbed Fe(III), leading to the formation of the same carbon-centred radical that is formed through the photo-Kolbe process (see Scheme 1). Fe(II) could be reoxidised to Fe(III) by reaction with holes or O_2 (although is not included, adsorption–desorption equilibria might also occur [23]):

$$> Ti^{IV}(Fe^{III}) - MA + h\nu \rightarrow > Ti^{IV}(Fe^{II}) + MA^{\bullet}$$
$$> Ti^{IV}(Fe^{II}) + h\nu(+O_2) \rightarrow > Ti^{IV}(Fe^{III}) + (O_2^{\bullet -})$$

Finally, several authors claim that the ability of Fe(III) to avoid the electron–hole pair recombination, due to the separation of the charge carrier species, would explain the enhanced photoactivity of some iron-doped TiO_2 samples [37,38]. Adsorbed Fe(III) can also play this role in the studied system. However, the different perspectives we have proposed concerning the Fe(III) role are not mutually exclusive but complementary to explain the results presented in this paper.

5. Conclusions

The Fe(III) adsorption over TiO_2 catalyst renders improved mineralization kinetics of maleic acid through a modified degradation pathway. In the TiO_2 + UV assays, malic, acrylic, malonic, oxalic, acetic and formic acids have been detected, whereas in the case of the TiO_2/Fe + UV

system malonic and formic acids are the only detected mineralization intermediates of maleic acid. The ATR–FT-IR results, along with the lack of salt effects on the behaviour of the TiO_2/Fe system, indicate that the Fe(III) effects are due to different surface phenomena. In one hand, the nature of the detected intermediates can be connected with enhanced adsorption and reactivity of O_2 related species. On the other hand, the presence of adsorbed Fe(III)–MA complexes might contribute to increased photocatalytic efficiency. Finally, the lower *cis–trans* isomerization yields could be taken to mean that Fe(III) loading decrease the geminate recombination yields.

The faster and cleaner mineralization pathway of maleic acid, the lack of salt effects, and the possibility of an easy recovery and reuse of the catalyst, without lowering the increased efficiency, makes the Fe(III) adsorption a useful strategy of TiO_2 modification.

Acknowledgements

The authors wish to thank to CICYT (project no. PPQ2002-04060-C02-01), EC(CADOX PROJECT) and UAB (M.I.F. PhD grant) for financial support.

References

[1] D.F. Ollis, H. Al-Ekabi (Eds.), Photocatalytic Purification and Treatment of Water and Air, Elsevier, Amsterdam, 1993.
[2] A. Mills, S. LeHunte, J. Photochem. Photobiol. A 108 (1997) 1.
[3] D.M. Blake, Bibliography of Work on Photocatalytic Removal of Hazardous Compounds from Water and Air, National Renewable Energy Laboratory, Golden, 1997.
[4] P.T. Anastas, J.C. Warner, Green Chemistry: Theory and Practice, University Press, Oxford, 1998.
[5] D.F. Ollis, Photochemical Conversion and Storage of Solar Energy, Kluwer Academic Publishers, Dordrecht, 1991, p. 593.
[6] M. Martha, W.F. Jardim, Catal. Today 76 (2002) 201.
[7] M. Grätzel, K. Kalyanasundaram, in: M. Grätzel, K. Kalyanasundaram (Eds.), Photosensitization and Photocatalysis using Inorganic and Organic Compounds, Kluwer Academic Publishers, 1993.
[8] B.O. Regan, M. Grätzel, Nature 353 (1991) 737.
[9] A. Assabane, Y. Ait, H. Tahiri, C. Guillard, J.M. Herrmann, Appl. Catal. B 24 (2000) 71.
[10] C. Pulgarin, N. Adler, P. Péringer, C. Comninellis, Water Res. 28 (1997) 887.
[11] A.D. Weisz, L. García Rodenas, P.J. Morando, A.E. Regazzoni, M.A. Blesa, Catal. Today 76 (2002) 103.
[12] X. Li, J.W. Cubbage, W.S. Jenks, J. Org. Chem. 64 (1999) 8525.
[13] C. Bouquet-Somrani, A. Finiels, P. Graffin, J-L. Olive, Appl. Catal. B 8 (1996) 101.
[14] X. Li, J.W. Cubbage, T.A. Tetzlaff, W.S. Jenks, J. Org. Chem. 64 (1999) 8509.
[15] T.R. Felthouse, 4th ed. Kirk-Othmer Encyclopedia of Chemical Technology, vol. 15, Wiley, 1995 p. 893.
[16] S. Budavari (Ed.), The Merck index: An Encyclopedia of Chemicals, Drugs, and Biologicals, 12th ed. Merck and Co. Inc., 1996, p. 973.
[17] M.I. Franch, J.A. Ayllón, J. Peral, X. Domènech, Catal. Today 76 (2002) 221.
[18] M.I. Franch, J.A. Ayllón, J. Peral, X. Domènech, Appl. Catal. B 50 (2004) 89.
[19] T.D. Waitejkvhj, Re/Views Environ. Sci. Bio/Technol. 1 (2002) 9.
[20] M.I. Litter, Appl. Catal. B 23 (1999) 89.
[21] A.E. Greenberg, L.S. Clesceri, A.D. Eaton, M.A.H. Franson (Eds.), Standard Methods for the Examination of Water and Wastewater, 18th ed. American Public Health Association, American Water Works Association, Water Environment Federation, Washington, 1992, p. 3.
[22] M.I. Litter, J.A. Navio, J. Photochem. Photobiol. A 98 (1996) 171.
[23] J. Araña, O. González Díaz, M. Miranda Saracho, J.M. Doña Rodríguez, J.A. Herrera Melián, J. Pérez Peña, Appl. Catal. B 36 (2002) 113.
[24] A. Nubile, M.W. Davis, J. Catal. 6 (1989) 383.
[25] J. Sima, J. Makanova, Coord. Chem. Rev. 160 (1997) 161.
[26] G.R. Bamwenda, H. Arakawa, Sol. Energy Mater. Sol. Cel. 70 (2001) 1.
[27] T.J. Strathmann, A.T. Stone, Environ. Sci. Technol. 36 (2002) 653.
[28] C. von Sonntag, H.-P. Schuchmann, Angew. Chem. Int. Ed. Engl. 30 (1991) 1229.
[29] J-M. Herrmann, H. Tahiri, C. Guillard, P. Pichat, Catal. Today 54 (1999) 131.
[30] Y-C. Oh, X. Li, J.W. Cubbage, W.S. Jenks, Appl. Catal. B 54 (2004) 105.
[31] T. Rajh, L.X. Chen, K. Lukas, T. Liu, M.C. Thurnauer, D.M. Tiede, J. Phys. Chem. B 106 (2002) 10543.
[32] K.D. Dobson, A.J. McQuillan, Spectrochim. Acta A 55 (1990) 1395.
[33] H. Al-Ekabi, P. de Mayo, J. Phys. Chem. 89 (1985) 5815.
[34] R.L. Jackson, M.R. Trusheim, J. Am. Chem. Soc. 104 (1982) 6590.
[35] M.I. Litter, B.C. Banmgartner, G.A. Urrutia, M.A. Blesa, Environ. Sci. Technol. 25 (1991) 1907.
[36] C. Guillard, C.F. Hoang-Van, P. Pichat, F. Marme, J. Photochem. Photobiol. A 89 (1995) 221.
[37] S-M. Oh, S-S. Kim, J.E. Lee, T. Ishigaki, D-W. Park, Thin Solid Films 435 (2003) 252.
[38] Z. Zhang, C-C. Wang, R. Zakaria, J.Y. Ying, J. Phys. Chem. B 102 (1998) 10871.